Luminescent and Redox Probes of Structure and Dynamics in Quaternized Poly(4-vinylpyridine) Films on Electrodes

Seung-Mo Oh and Larry R. Faulkner*

Contribution from the Department of Chemistry, University of Illinois, 1209 West California Street, Urbana, Illinois 61801. *Received October 17, 1988*

Abstract: The properties of partially quaternized poly(4-vinylpyridine) films have been studied by coordinatively attaching luminescent and redox probes to free pyridine units within the polymer. Samples were examined as thin films spin coated onto glass or electrodes. The luminescent moiety was $Re(CO)_3(phen)$ (phen = 1,10-phenanthroline). It showed properties that depended strongly on the identity of the anion in the supporting electrolyte adjacent to the film. The emission maximum shifted to the red, and the quantum yield decreased in the order dry film > 0.1 M $NaClO_4$ > 0.1 M potassium *p*-toluenesulfonate > 0.1 M KNO_3. The isotope effect caused by changing the solvent from H_2O to D_2O fell in the reverse order. The results show that the anion has a large impact on film structure. In nitrate the films are strongly hydrated, but in perchlorate they are dry and compact. The redox moiety was $Ru(bpy)_2Cl^{2+/1+}$. The activation energies for electron diffusion in the network of redox centers were assessed by temperature-resolved chronocoulometry. The activation energies were independent of the concentration of redox centers in the film but were ordered according to electrolyte as given above. They were roughly linearly dependent on the degree of chemical cross-linking. The permeabilities of the films to redox-active ions in solution were larger than the electron diffusion coefficients by an order of magnitude but were strongly dependent on the anion of the supporting electrolyte, inversely in the order given above. The results suggest that electron diffusion is controlled by segmental motions within the polymer and that the anion dependence is a structural effect.

It has been generally accepted that electron diffusion in electroactive films can be controlled by electron hopping between redox sites, by the short-range and long-range internal mobility of redox centers, or by barriers to the motions of charge-compensating ions, depending on the internal fluidity of the film and the facility of intersite electron transfer.[1] In a separate paper strongly related to this one,[2] we report studies of electron-transport dynamics in networks of $Fe(CN)_6^{3-/4-}$ centers that were electrostatically bound in partially quaternized poly(4-vinylpyridine) (QPVP) modified electrodes. It was proposed there that the short-range mobility of the QPVP matrix mainly controls electron diffusion in the system. Variable-temperature chronocoulometry was employed to measure the electron diffusion coefficients (D_E) and activation energies (E_a) for electron transport. The measured E_a steadily increased as the concentration of the $Fe(CN)_6^{3-/4-}$ was increased. We suggested that this trend reflects the tendency of the polymer matrix to become more cross-linked upon taking up the redox ions, resulting in a loss of short-range mobility. The observed D_E and E_a were strongly influenced by the anionic species in the background electrolyte. Separate experiments showed that the observed permeation rates of electroactive solutes were generally an order of magnitude larger ($\sim 10^{-7}$ cm^2/s) than the D_E values ($\sim 10^{-8}$ cm^2/s), hence we could eliminate the transport of supporting anions as a possible controlling factor for electron motion. The anion dependence was explained on the basis of structural alterations in the film caused mainly by ion-pair interactions[3] between the positively charged polymer matrix and the anionic species. Infrared and ionic conductivity measurements indicated that the QPVP matrix interacts particularly strongly with ClO_4^-. Successively weaker interactions apply as the anion is switched to *p*-toluenesulfonate (OTs^-) and then to NO_3^-.

In this paper, we deal with QPVP films in which molecular probes have been attached coordinatively to the polymer. First, a luminescent inorganic complex was attached to the QPVP by coordination of free pendant pyridine units to the $Re(CO)_3(phen)$ moiety. The polymer-bound Re(I) complex was stable in aqueous solution and showed fluorescent properties that were affected by the anionic species. The results are consistent with the conclusions from the QPVP–$Fe(CN)_6^{3-/4-}$ system, in that they confirm anion-induced alterations in the structure and state of hydration of the film. These luminescence experiments are particularly valuable, because they show that the structural alterations affect the immediate local environment of the probes. Other studied properties[2] reflect the mean properties of the polymeric phase, which could differ from the local environments at coordinated transition-metal centers, if the polymer exhibited domainlike substructure with interspersed rigid and fluid regions.

Also presented here are studies of the electron-transport dynamics for networks of $Ru(bpy)_2Cl^{2+/1+}$ moieties that were coordinatively bound to free pyridine units of the QPVP. Related work has just been reported by Lyons et al.,[4] who examined this redox center in cross-linked, protonated PVP. For such systems, the discussion of electron-transport dynamics can be simplified, since the physical diffusion of the redox centers can be eliminated as a possible controlling factor for electron transport. The results with films that were chemically cross-linked to different degrees clearly suggest that segmental motion of the polymer controls the rate of electron diffusion.

Experimental Section

Materials. Partially quaternized polyvinylpyridine (QPVP) was prepared as reported elsewhere.[2,5] The sample was 63% quaternized.

The polymer-bound complex $[(QPVP)Ru(bpy)_2Cl]Cl$ (bpy = 2,2′-bipyridine) was prepared as described in the literature,[6] with QPVP/Ru ratios of 80:1 to 4:1 based on the unquaternized pyridine unit in the QPVP. A methanolic solution of QPVP and *cis*-$Ru(bpy)_2Cl_2$ (Aldrich Chemical Co.) was refluxed for 3 days. After being filtered, the resulting solution was concentrated, and the polymer was precipitated with ethyl ether. The product was purified by dissolution in methanol and reprecipitation with ethyl ether several times, and then it was dried in vacuum for 1 day. The concentration of the polymer-bound $Ru(bpy)_2Cl$ was determined, after spin coating on a glassy carbon electrode (geometric area = 0.283 cm^2), by integrating the area under the oxidation peak in cyclic voltammetry at 2 mV/s. The film thickness was measured by an Alpha-step profilometer (Tencor Corp.) as described previously.[2] In calculating concentrations, the dry film thickness (6500 Å) was used.

The complexes $[(py)Re(CO)_3(phen)]X$ and $[(QPVP)Re(CO)_3(phen)]X$ (py = pyridine, phen = 1,10-phenanthroline, and X = anion)

* To whom correspondence should be addressed.

(1) The literature is reviewed extensively in ref 2.
(2) Oh, S. M.; Faulkner, L. R. *J. Electroanal. Chem.*, in press.
(3) (a) Miller, M. L. *The Structure of Polymers*; Reinhold: New York, 1966; Chapter 12. (b) Eisenberg, A.; King, M. *Ion-Containing Polymers*; Academic Press: New York, 1977.
(4) Lyons, M. E. G.; Fay, H. G.; Vos, J. G.; Kelly, A. J. *J. Electroanal. Chem.* **1988**, *250*, 207.
(5) Braun, H.; Storck, W.; Doblhofer, K. *J. Electrochem. Soc.* **1983**, *130*, 807.
(6) (a) Clear, J. M.; Kelly, J. M.; Pepper, D. C.; Vos, J. G. *Inorg. Chim. Acta* **1979**, *33*, L139. (b) Haas, O.; Vos, J. G. *J. Electroanal. Chem.* **1980**, *113*, 139. (c) Haas, O.; Kriens, M.; Vos, J. G. *J. Am. Chem. Soc.* **1981**, *103*, 1318.

0002-7863/89/1511-5613$01.50/0

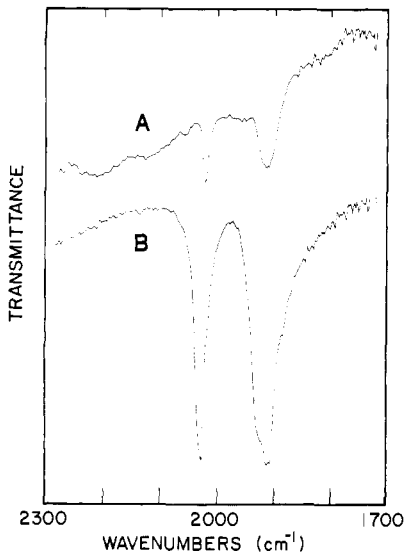

Figure 1. IR spectra in the CO stretching region: (A) $[(QPVP)Re(CO)_3(phen)]^+CF_3SO_3^-$; (B) $[(py)Re(CO)_3(phen)]^+CF_3SO_3^-$.

were prepared according to a modified version of the reported method.[7] The starting material, $ClRe(CO)_3(phen)$ was synthesized[8] by heating a 2:1 mole ratio of 1,10-phenanthroline and $ClRe(CO)_5$ (Pressure Chemical Co.) to 60 °C in benzene solution. The yellow solid product was recrystallized from CH_2Cl_2 by addition of *n*-pentane. For the preparation of $[(py)Re(CO)_3(phen)]CF_3SO_3$, 0.097 g (0.2 mmol) of $ClRe(CO)_3(phen)$ and 0.062 g (0.24 mmol) of Ag CF_3SO_3 were dissolved in 100 mL of solution. The reaction mixture was refluxed for four days. After removal of the AgCl by centrifuging several times, the resulting solution was completely dried by rotary evaporation. The yellow solid mixture was dissolved in a minimum amount of CH_3CN, from which the solid impurities were filtered off. The final product was precipitated by adding a 1:1 mixture of ethyl ether and N-pentane to the resulting solution. Elemental analysis: Calcd C, 37.17; H, 1.93; N, 6.19; S, 4.72. Found: C, 37.37; H, 1.84; N, 6.44; S, 4.69.

For the preparation of QPVP-bound Re(I) complex, $ClRe(CO)_3(phen)$, $AgCF_3SO_3$ was dissolved in CH_3CN and refluxed for 4 days. The resulting AgCl precipitate was filtered off and further removed from the solution by centrifugation. The resulting solution was concentrated, and the QPVP complex was precipitated by addition of ethyl ether. The polymeric product was further purified by reprecipitation from methanol with ethyl ether and was dried under vacuum for 1 day. The characteristic ν_{CO} of the $[(QPVP)Re(CO)_3(phen)]^+$ complex was well matched with that for $[(py)Re(CO)_3(phen)]^+$ (Figure 1). The mole ratio of free pyridine units to derivatized ones was 8.4.

$NaFe(edta)\cdot 3H_2O$ (edta = ethylenediaminetetraacetate) was prepared and purified according to a procedure in the literature.[9] All other chemicals were reagent grade and were used without further purification.

The film preparation, variable-temperature chronocoulometry, and permeability measurements were carried out with equipment and techniques described in our related paper.[2]

Luminescence measurements were performed with a SPEX 212 fluorescence spectrometer at right-angle geometry. A semicircular spectroelectrochemical cell was mounted on a vernier dial to allow a variable angle of incidence for the excitation beam on the electrode surface. Spectra were normally obtained with 0.5-nm resolution and 0.5-s integration at each data point. For the measurements of solutions, a 1-cm quartz cuvette was used. For measurements of films, the QPVP–Re(I) complex was deposited on a glass slide (1 in. × 1 in.) by spin coating. The dry film thickness was ~2 μm. Measurements of dry films were done in air. For measurements in aqueous solutions of salts, the film-deposited glass slide was inserted in a spectroelectrochemical cell that was filled with a nitrogen-bubbled aqueous solution.

Results and Discussion

Luminescence Properties of $[(QPVP)Re(CO)_3(phen)]CF_3SO_3$ Films. A series of fac-$[SRe(CO)_3L]^+$ complexes (S = CH_3CN, pyridine, or piperidine and L = 1,10-phenanthroline, 2,2′-bipyridyl, or 2,2′-biquinoline) are known to have multiple emission characteristics.[7,10] The spectra at 77 K comprise two emissions: a metal-to-ligand [Re → π*(phen)] charge transfer (MLCT) at lower energy and π → π*(phen) intraligand transition at higher energy. Emission lifetimes at 77 K for these states are reported to be 11 and 75 μs, respectively. The emission spectra are dominated by the MLCT emission to an increasing degree at higher temperatures, and the observed emission at 298 K is essentially completely due to the MLCT transition.[7] The lowest excited state of $[(py)Re(CO)_3(phen)]^+$ is associated with a Re → phen MLCT transition in absorption [$\lambda_{max} \sim 365$ nm ($\epsilon \sim 4800$ M^{-1} cm^{-1}) in CH_3CN]. It is emissive [$\lambda_{max} \sim 552$ nm, $\tau \sim 0.8$ μs] in CH_3CN solution at 298 K.[7]

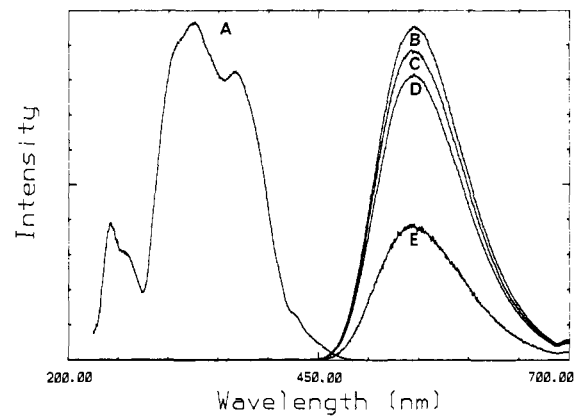

Figure 2. Uncorrected excitation (A) and emission spectra (B–E) for 0.15 mM $[(py)Re(CO)_3(phen)]^+CF_3SO_3^-$ in H_2O. Curve A is for emission at 545 nm. Curves B–E are for excitations at 242, 307, 325, and 368 nm, respectively.

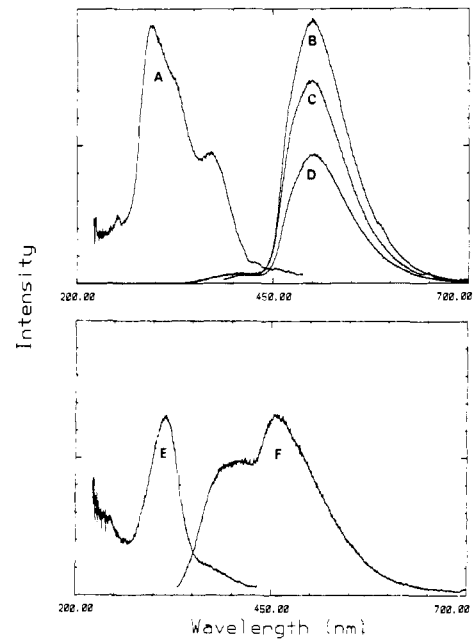

Figure 3. Uncorrected excitation (A) and emission (B–D) spectra for a dry $[(QPVP)Re(CO)_3(phen)]^+CF_3SO_3^-$ film deposited on glass slides. The film thickness was ~2 μm. Curve A is for emission at 500 nm. Curves B–D are for excitations at 297, 325, and 358 nm. Uncorrected excitation (E) and emission (F) spectra for QPVP film deposited on a glass slide. Curve E is for emission at 450 nm. Curve F is for excitation at 316 nm. The two sets of spectra are not on a common scale.

(7) Fredricks, S. M.; Luong, J. C.; Wrighton, M. S. *J. Am. Chem. Soc.* **1979**, *101*, 7415.
(8) Wrighton, M. S.; Morse, D. L. *J. Am. Chem. Soc.* **1974**, *96*, 998.
(9) Sawyer, D. T.; McKinnie, J. M. *J. Am. Chem. Soc.* **1960**, *82*, 4191.
(10) (a) Luong, J. C.; Nadjo, L.; Wrighton, M. S. *J. Am. Chem. Soc.* **1978**, *100*, 5790. (b) Summers, D. P.; Luong, J. C.; Wrighton, M. S. *J. Am. Chem. Soc.* **1981**, *103*, 5238. (c) Caspar, J. V.; Meyer, T. J. *J. Phys. Chem.* **1983**, *87*, 952. (d) Reitz, G. A.; Dressick, W. J.; Demas, J. N.; DeGraff, B. A. *J. Am. Chem. Soc.* **1986**, *108*, 5344. (e) Lees, A. J. *Chem. Rev.* **1987**, *87*, 711.

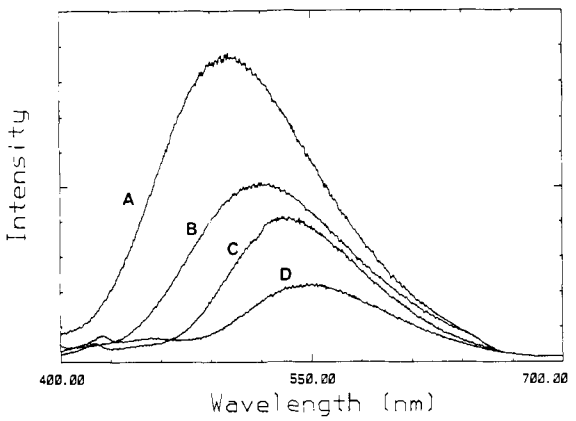

Figure 4. Uncorrected emission spectra for $(QPVP)Re(CO)_3(phen)^+$ films (dry thickness, ~2 μm) deposited on glass slides. All spectra are for excitation at 368 nm: (A) dry film in air; (B) immersed in 0.1 M $NaClO_4$; (C) immersed in 0.1 M KOTs; and (D) immersed in 0.1 M KNO_3. The shapes of spectra are independent of excitation wavelength.

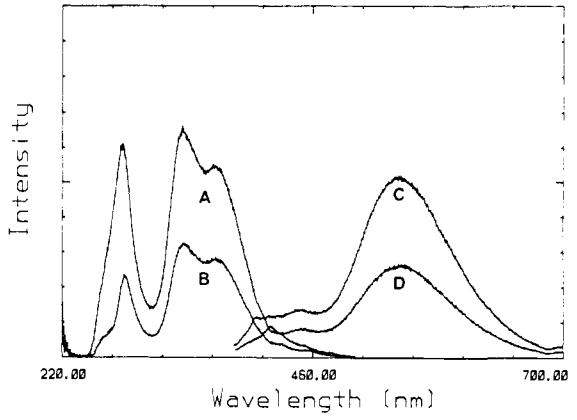

Figure 5. Uncorrected excitation and emission spectra for $(QPVP)Re(CO)_3(phen)^+$ films immersed in 0.1 M KNO_3 in H_2O (B, D) and D_2O (A, C). Spectra A and B are for excitation of emission at 543 nm. Spectra C and D are for emission excited at 368 nm.

Figure 2 shows the excitation (A) and emission (B–E) spectra for an aqueous solution of $[(py)Re(CO)_3(phen)]^+CF_3SO_3^-$. The four emission spectra (B–E) are excited at wavelengths corresponding to the four absorption maxima in the excitation spectrum (A). The excitation spectrum (emission wavelength = 545 nm) shows multiple absorption features. The lowest excited state, arising in absorption at 368 nm, can be assigned to the MLCT transition on the basis of the literature.[7] The absorptions at higher energies (307, 325 nm) would then be related to intraligand (phen) transitions. The emission spectra are featureless and are independent of the excitation wavelength over the range 242–368 nm. The emission maximum in H_2O (545 nm) is close to the literature value for CH_3CN (552 nm).

Figure 3 displays the excitation (A) and emission (B–D) spectra for a dry film of $[QPVPRe(CO)_3(phen)]^+CF_3SO_3^-$ deposited on glass slides. The higher energy absorptions in the excitation spectrum are more prominent than in the spectrum of the aqueous solution of $[(Py)Re(CO)_3(phen)]^+$. This increase comes from the QPVP (see Figure 3E,F). The emission spectra (B–D) remain featureless and independent of the excitation wavelength. Very weak emission assignable to QPVP can be seen in the range of 400 nm. Curves E and F confirm that QPVP has emissions near that wavelength. This emission does not contribute appreciably to the observations that follow.

To investigate changes in the QPVP structure upon exposure to different anions, the Re(I)-labeled QPVP films were soaked in aqueous solutions of KNO_3, potassium *p*-toluenesulfonate (KOTs), and $NaClO_4$. Figure 4 shows the emission spectra for dry (A) and soaked (B–D) films. The intensity and emission maximum are clearly anion dependent. The possibility that the anion dependence reflects a specific interaction between the Re(I) complex and the anion could be excluded by the fact that the $[(py)Re(CO)_3(py)]X$ complex shows an emission intensity in solution that is independent of the anion of concern here, at least at 0.1 M concentrations. The long lifetime of the complex ensures that, under such conditions, each excited species will encounter anions an average of roughly 1000 times before decay. Since there is no appreciable quenching of luminescence by the anions, the anion dependence of luminescence efficiency must be assigned to changes in local environment arising from interactions between the QPVP matrix and the anion.

We suggest in our related paper[2] that a QPVP film has a structure that is strongly influenced by the anion. It apparently is compact when neutralized with perchlorate but becomes more fluid when neutralized with *p*-toluenesulfonate or nitrate. As can be seen in Figure 4, the MLCT emission intensity for the film-bound Re(I) complex decreases in the order of $ClO_4^- > OTs^- > NO_3^-$. This anion-dependent fluorescence intensity of the Re(I) complex in QPVP film follows the order of rigidity of the QPVP films, as assessed by the activation energies for electron diffusion among ferri/ferrocyanide.[2]

Table I. Luminescence Properties of Re(I) Complex

	isotope effect[a]	emission max/nm
$[(py)Re(CO)_3(phen)]^+$ in H_2O	1.56	545
$[(QPVP)Re(CO)_3(phen)]^+$		
in 0.1 M KNO_3	1.97	543
in 0.1 M KOTs	1.24	534
in 0.1 M $NaClO_4$	1.12	520
in dry film		500

[a] Ratio of emission intensity at the spectral maximum in D_2O vs H_2O.

Related results have been reported for luminescence in other media. The luminescence characteristics of $ClRe(CO)_3(phen)$ depend significantly on the environment; longer lived and more intense emission has been observed in rigid polyester resins or in glasses at 77 K as compared to fluid solutions at room temperature.[8] These effects have been attributed to a decrease in the rate of nonradiative deactivation in rigid media.

A particularly useful aspect of this complex is its sensitivity to water in the immediate environment. The presence of OH oscillators is known to provide an efficient pathway for nonradiative deactivation through energy transfer to OH vibrational overtones.[11] It is generally accepted that the rate of deactivation via this process is directly proportional to the number of OH oscillators in the first solvation sphere.[11] Since OD oscillators are much less efficient in effecting this deactivation process, the radiationless decay exhibits a large isotope effect.

The isotope effect can be exploited in our system to gain insight into the anion-induced structural changes. As can be seen in Figure 5, the excitation and emission intensity of a film exposed to nitrate depends strongly on the solvent employed. With D_2O, the efficiency of emission was roughly double that observed with H_2O. Similar intensity variations can be seen in the other salt solutions (Table I). The isotope effect is large in KNO_3 but decreases sharply in the presence of the other salts.

The isotope effect in this system can be explained readily on the basis of water contents inside the QPVP films. It is clear that $QPVP^+NO_3^-$ absorbs many more water molecules than $QPVP^+ClO_4^-$ film. In fact the isotope effect for $QPVP^+ClO_4^-$ suggests that the films neutralized with perchlorate are nearly dry.

Another clear feature in Figure 4 is that the emission maximum of the MLCT depends on the anionic species in the matrix. Table I provides the maxima. The Re(I) complex bound to $QPVP^+ClO_4^-$

(11) (a) Kropp, J. K.; Windsor, M. W. *J. Chem. Phys.* **1963**, *39*, 2769. (b) Kropp, J. L.; Windsor, M. W. *J. Chem. Phys.* **1966**, *45*, 761. (c) Kropp, J. L.; Windsor, M. W. *J. Phys. Chem.* **1967**, *71*, 477. (d) Haas, Y.; Stein, G. *J. Phys. Chem.* **1971**, *75*, 3677. (e) Horrocks, W. DeW., Jr.; Sudnick, D. K. *J. Am. Chem. Soc.* **1979**, *101*, 334.

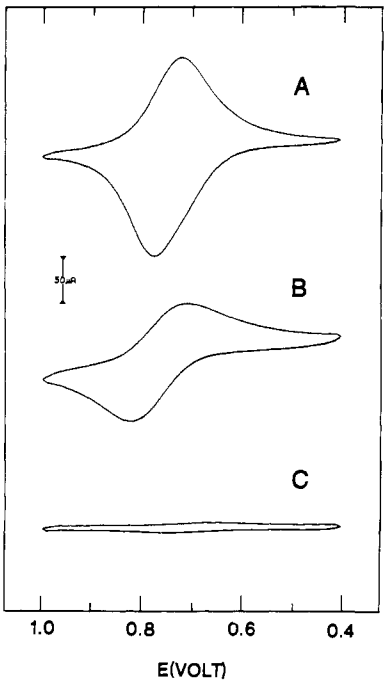

Figure 6. Cyclic voltammograms of QPVP–$Ru(bpy)_2Cl^{2+/1+}$ deposited on glassy carbon electrodes in different background electrolytes. The concentration of $Ru(bpy)_2Cl^{1+}$ moieties was $\sim 5 \times 10^{-4}$ mol/cm^3 based on the dry film thickness (6500 Å): (A) in 0.1 M KNO_3; (B) in 0.1 M KOTs; (C) in 0.1 M $NaClO_4$. Scan rate = 50 mV/s, T = 23 °C. Reference electrode was Ag/AgCl/KCl (3.5 M).

shows the highest energy emission (520 nm), with a maximum close to that for the dry film (500 nm), while the luminescent probe in $QPVP^+ NO_3^-$ gives rise to an emission at 543 nm, a maximum close to that (545 nm) of the aqueous solution of $[(py)Re(CO)_3(phen)]^+$. Thus, the anion-dependent position of the emission maximum can also be explained on the basis of water sorbed by the QPVP films. This result may reflect changes in the shape of the excited-state potential well. That is, the MLCT excited state of the Re(I) complex might be more stable in a polar medium, since the excited state can be stabilized via dipolar interactions with the surrounding water molecules.

Electron Transport in [(QPVP)Ru(bpy)$_2$Cl]Cl. The *cis*-$Ru(bpy)_2Cl_2$ complex (bpy = 2,2′-bipyridyl) can be attached to the pyridine moiety of the partially quaternized poly(4-vinylpyridine). The polymer-bound Ru(II) complex is stable in contact with aqueous solutions of salt.

In cyclic voltammetry, the peak current depends on the QPVP/Ru(II) ratio in the polymer, and the attached Ru(II) complex shows the electrochemical behavior expected for a surface-confined species: a symmetrical voltammetric shape and a linear dependence of the peak current on the scan rate. Also, the leaching rate of the $Ru(bpy)_2Cl^{2+/1+}$ is much smaller than that of the electrostatically bound $Fe(CN)_6^{3-/4-}$ complex.

Figure 6 presents the voltammograms for the QPVP-bound $Ru(bpy)_2Cl^{2+/1+}$ couple in three different background electrolytes. In 0.1 M KNO_3, the voltammogram is well developed; yet the peaks are almost invisible in 0.1 M $NaClO_4$. The well-developed voltammograms can be reproduced when the electrode is moved back to KNO_3 solution. This illustrates that the Ru(II) complex is not decomposed or leached out from the polymer film upon exposure to perchlorate. The Ru(II) complexes remain bound, but the electron-transport rate becomes very small in $QPVP^+$-ClO_4^-.

Figure 7 presents the activation energies for electron transport in QPVP–Ru(II) films. They were obtained from variable-temperature chronocoulometry experiments in two different background electrolytes. The activation energies in 0.1 M KNO_3 solution (5–7 kcal/mol, 20–30 kJ/mol) are considerably smaller than those measured in 0.1 M K KOTs (8–14 kcal/mol, 33–60 kJ/mol). The activation energies in KCl were similar to those

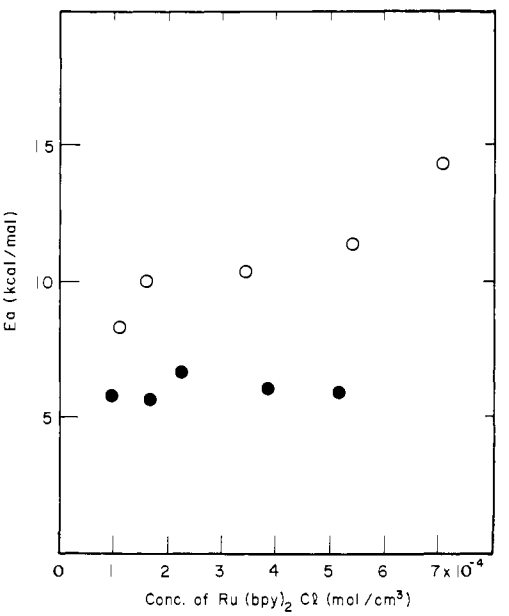

Figure 7. Activation energies for electron diffusion vs the concentration of coordinatively bound $Ru(bpy)_2Cl^{1+/2+}$ in QPVP. Open circles, 0.1 M KOTs; filled circles, in 0.1 M KNO_3. Film thickness was assumed to be 6500 Å. Electrode area was 0.283 cm^2. The QPVP film was 4% cross-linked. The concentration of $Ru(bpy)_2Cl^{2+/1+}$ was estimated by integrating the area under the oxidation peak in cyclic voltammetry at 2 mV/s.

Table II. Anion-Dependent Electrochemical Properties[a]

background electrolyte	E_a/ (kcal mol^{-1})[b]	$10^9 D_E$/ (cm^2 s^{-1})[c]	$10^6 D_S\kappa$/ (cm^2 s^{-1})[d]
0.1 M KNO_3	5.7	5.3	2.3 (5.0)
0.1 M KCl	5.5	5.4	2.1 (5.1)
0.1 M KOTs	9.9	1.2	0.98 (4.5)
0.1 M $NaClO_4$			0.0095 (4.3)

[a] Films were 4% cross-linked, and film thickness was ~6500 Å. [b] [Ru(II)] = 1.6×10^{-4} mol/cm^3. [c] [Ru(II)] = 2.1×10^{-4} mol/cm^3. [d] The electroactive solute was 0.4 mM $Fe(edta)^-$. Concentration of $Ru(bpy)_2Cl$ was 2.1×10^{-4} mol/cm^3. Parentheses contain diffusion coefficients for $Fe(edta)^-$ in the aqueous electrolyte as measured at a naked glassy carbon electrode by hydrodynamic voltammetry.

in KNO_3 (Table II). Because the electrochemical response was so weak in the presence of $NaClO_4$, no activation energy could be measured for that system. A similar anion dependence was found for QPVP containing the $Fe(CN)_6^{3-/4-}$ couple, as described in our related paper.[2]

Lyons et al.[4] have recently reported activation energies for D_E in one system very similar to ours, viz., PVP labeled with $Ru(bpy)_2Cl^{2+/1+}$ and immersed in 0.05 M Na_2SO_4. They measured E_a = 40 kJ/mol, which is comparable to the value we observe in nitrate media. They went on to examine copolymers with methyl methacrylate and vinylpyridine (labeled with $Ru(bpy)_3Cl^{2+/1+}$) in acidic media, including $HClO_4$. There was a rise in activation energy from 32 kJ/mol in 0.05 H_2SO_4, to 36 kJ/mol in 0.1 M HCl, to 43 kJ/mol in 0.1 $HClO_4$. This trend probably manifests the structural changes that we observe, but the trend is much weaker than in our systems.

Table II also presents the permeation rates of $Fe(edta)^-$ through the QPVP–$Ru(bpy)_2Cl^{1+/2+}$ films in various electrolytes. Permeation rates are defined here as $D_S\kappa$, where D_S is the diffusion coefficient for the permeating solute in the film and κ is the partition coefficient controlling the concentration of the solute in the film. The permeation rates were measured, as in our earlier work,[2] from the intercepts of Koutecky-Levich plots for the limiting current for reduction of $Fe(edta)^-$ at a film-covered electrode. The permeation rate ($D_S\kappa$) of $Fe(edta)^-$ was not far below the value for aqueous solution when the film was exposed to 0.1 M KNO_3, but it decreased significantly in KOTs and sharply in $NaClO_4$.

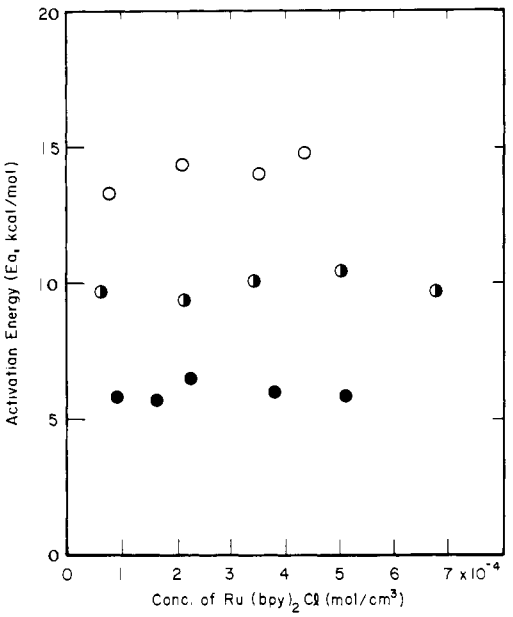

Figure 8. Activation energies from variable-temperature (0–25 °C) chronocoulometry on QPVP–$Ru(bpy)_2Cl^{2+/1+}$ films deposited on glassy carbon electrodes. The background electrolyte was 0.1 M KNO_3. The QPVP film was cross-linked in different degrees: Filled circles, 4%; half-filled circles, 8%; open circles, 12%. Experimental conditions were as described in Figure 7.

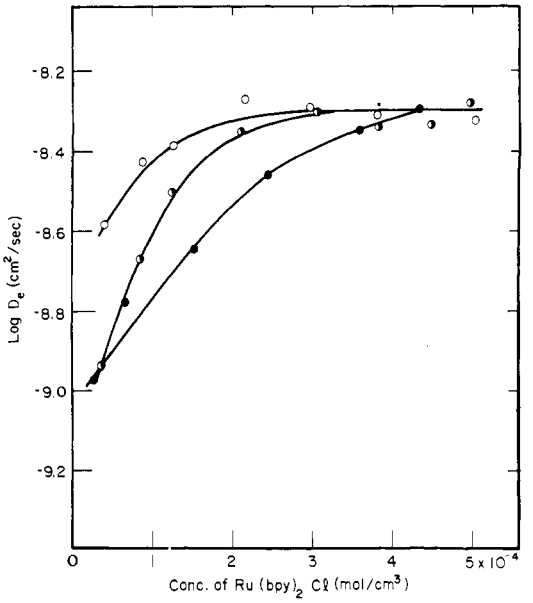

Figure 9. Electron-diffusion coefficients measured by chronocoulometry vs the concentration of $Ru(bpy)_2Cl^{2+/1+}$ in QPVP film. Open circles, 4% cross-linked; half-filled circles, 8% cross-linked; filled circles, 12% cross-linked.

Our values of permeation rate are derived from a model featuring the film as a uniformly permeable barrier. It is not simple to distinguish this case from the situation in which permeation occurs through pinholes.[12] We discuss the problem of interpretation in greater detail in our related paper.[2] For our purposes here, we can point out that the measured permeation rates for films in nitrate solution would require roughly 50% of the surface area to be pinholes. In perchlorate, the pinhole fraction would then be less than 1%. Both the magnitude of the required fraction in nitrate and the magnitude and direction of change in going to perchlorate render an interpretation in terms of pinholes less tenable than one based on a uniform barrier. Of course, it is possible that the system is dominated by uniform permeation in nitrate and by pinholes in perchlorate.

In any case, the permeation rates reflect an anion-dependent structure in the film. Upon comparing them with the electron diffusion coefficients (D_E) listed in Table II, one sees that the permeation rates ($\sim 10^{-7}$ cm^2/s) are uniformly higher than the corresponding electron diffusion rates ($\sim 10^{-8}$–10^{-9} cm^2/s). If our view of the film as a uniformly penetrable barrier is correct, then the anion dependence of D_E does not reflect limitations on motions of the counterion in the matrix.

We therefore reach conclusions consistent with those of our related paper[2] with respect to the anion dependence of electron diffusion, i.e., that the dependence arises from anion-induced changes in film structure. The electron-transport dynamics seem to be mainly controlled by the short-range mobility of the polymer matrix, which is influenced by ion-pair interactions between the polymer matrix and the anionic species.

Effects of Cross-Linking. One can gain a considerably enhanced view of the mechanism for electron diffusion by examining the effect of cross-linking, because variations in cross-linking afford systematic control of local rigidity. Figure 8 illustrates the effect of cross-linking on activation energies for electron diffusion in QPVP–Ru(II) films in aqueous of 0.1 M KNO_3. The concentration of the electroactive Ru(II) complex was changed by varying the QPVP/Ru ratio during the preparation of the QPVP–Ru(II) polymer as described in the Experimental Section. Three different degrees of cross-linking were employed (4%, 8%, and 12% based on the fraction of pyridine units in the QPVP). The activation energies depend on the degree of cross-linking (6–7 kcal/mol for 4% cross-linked film, 9–11 kcal/mol for 8% cross-linked QPVP, and 13–15 kcal/mol for 12% cross-linked film). However, the E_a does not depend appreciably on the concentration of the Ru(II) couple in the QPVP film. This behavior contrasts with that of the QPVP–$Fe(CN)_6^{3-/4-}$ system,[2] where E_a rose significantly with the concentration of $Fe(CN)_6^{3-/4-}$. This rise was attributed to the electrostatic cross-linking effect involving the positively charged polymer matrix and the multiply charged negative ions, $Fe(CN)_6^{3-/4-}$. Obviously there is no electrostatic cross-linking here, since $Ru(bpy)_2Cl^{2+/1+}$ is positively charged; hence the independence of E_a on the concentration of the Ru(II) complex is readily understood.

Figure 9 shows electron diffusion coefficients (D_E) as functions of the concentration of $Ru(bpy)_2Cl^{2+/1+}$ in QPVP film. The polymer films were cross-linked in the three different degrees. A similar trend in D_E versus concentration of Ru(II) can be seen in the three QPVP-$Ru(bpy)_2Cl$ films: D_E increases as the concentration of the $Ru(bpy)_2Cl$ increases and approaches a common limiting value near 5×10^{-9} cm^2/s. Since the E_a values clearly differ markedly (Figure 8) for the various degrees of cross-linking throughout the range of concentrations covered in Figure 9, we interpret the apparently common limit as fortuitous. However, the concentration of Ru(II) where the D_E approaches the limiting values is increased as the film becomes more cross-linked.

This behavior can be understood qualitatively by the following argument. First, we recognize that the activation energy does not change as the loading level increases (at constant cross-linking), hence the rate-determining process for electron diffusion does not change in character as the loading level changes. Since E_a depends practically linearly on the degree of cross-linking, segmental motion of the polymer, leading to local diffusion of the pendant group, seems to be always the rate-controlling element. The data sets in Figure 9 have a regime at low loading, where D_E sharply rises with load, and a regime at high loading, where D_E is nearly independent of load. The transition occurs roughly at the point where the concentration of redox centers roughly equals the cross-link concentration. Thus one can characterize the low-load regime as that where each redox center is likely to have a cross-link at a closer distance than the nearest-neighboring redox center. Conversely, the high-load regime corresponds to the zone where the nearest neighboring redox center generally lies inside the nearest cross-link. At a crude level, we can consider the system to consist of a network of cages defined by the cross-links. In the

(12) White, H. S.; Leddy, J.; Bard, A. J. *J. Am. Chem. Soc.* **1982**, *104*, 4811.

low-load regime, nearest-neighboring redox centers would be in adjacent cages, but in the high-load regime, they would be in the same cage. The independence of D_E on load in the high-load regime suggests that there is no advantage to the placement of nearest neighbors in a common cage. The rate limitation defining D_E seems to be imposed by the transfer of electrons from cage to cage, which requires exercising the cross-links. The high dependence of D_E on concentration in the low-load regime would then be understood in terms of the probability that adjacent cages are occupied with redox centers. The quantitative implications of these ideas are now under study.

Acknowledgment. We are grateful to the National Science Foundation for supporting this work under Grant 86-07984.

Polymerized Monolayers of Single-, Double-, and Triple-Chain Silane Amphiphiles and Permeation Control through the Monolayer-Immobilized Porous Glass Plate in an Aqueous Solution[1,2]

Katsuhiko Ariga and Yoshio Okahata*

Contribution from the Department of Polymer Chemistry, Tokyo Institute of Technology, Ookayama, Meguro-ku, Tokyo 152, Japan. *Received January 3, 1989*

Abstract: Single-chain ($C_{18}Si$), double-chain ($2C_{18}Si$), and triple-chain ($3C_{18}Si$) amphiphiles having triethoxysilane head groups were prepared. A monolayer of dialkylsilane amphiphiles ($2C_{18}Si$) could be polymerized to form a Si–O–Si linkage at the air–water interface on the acidic subphase of pH 2. The polymerized monolayer was easily transferred on a porous glass plate (average pore size 5 nm) by the Langmuir–Blodgett technique and could be covalently bonded with Si groups on the glass surface. Permeation of NaCl and water-soluble fluorescent probes (NQ_1) through the porous glass plate was controlled by a phase transition of the immobilized lipid monolayer. When the single-chain $C_{18}Si$ and the triple-chain $3C_{18}Si$ monolayers were immobilized on a porous glass plate, these monolayers hardly acted as a gate membrane for permeation. This is because, in the case of the single-chain $C_{18}Si$ monolayer, the polymerization on the subphase decreased the molecular packing of the monolayer and the polymerized monolayer could not be well transferred on the porous glass plate. Silane groups of the triple-chain amphiphile ($3C_{18}Si$) could not be polymerized in the monolayer because of the bulkiness of three alkyl chains, and the monomeric monolayer could not be transferred with a good transfer ratio on the substrate.

Permeability controllable, lipid-immobilized membranes have been developed as models to study the transport properties of biological membranes.[3-7] We have reported that signal-receptive, permeability-controllable, multibilayer-corked nylon capsule membranes[8] and multibilayer-immobilized polyion complex films,[9] where the multibilayers act as a gate membrane responding to external stimuli. These multibilayer-immobilized systems are easily prepared and physically stable for permeation membranes, which show clear physicochemical properties of a lipid bilayers. However, they are too thick (1–100 μm) compared with a single bilayer structure of biological membranes (5–7 nm) and are thought to have some defects in fine structures at interbilayers.

The Langmuir–Blodgett (LB) technique[10,11] transferring lipid monolayers from a water surface is well-known to prepare well-oriented ultrathin films in a molecular level on a substrate. Recently, LB multilayer films supported on a porous substrate have been utilized for filtration purposes, e.g., for ion permeation, pervaporation, and gas separation.[12-19] However, for the utilization of LB films as permeability-controllable membranes in an aqueous phase, we should consider whether the LB films are swollen between interlayers and are stable for flaking in an aqueous solution at harsh conditions (at a high temperature or a high ionic strength) or not.

In this paper, we prepare silane-functionized monolayer-forming amphiphiles having single, double, and triple alkyl chains and polymerize their Langmuir monolayers with a Si–O–Si linkage on a water subphase, which are immobilized covalently on a porous glass plate by LB techniques (see Figure 1). The lipid monolayer immobilized on a porous glass plate acts as a gate membrane for permeations of ions and water-soluble fluorescent probes responding to the phase transition from solid to liquid crystalline state of the lipid monolayer. This is the first study to control the permeability with the thinnest (2 nm) lipid monolayer film. Sagiv

* To whom all correspondence should be addressed.

(1) Permeability Controllable Membranes. 11. Part 10 of this series: Okahata, Y.; Shimizu, A. *Langmuir*, in press.

(2) Preliminary report: Okahata, Y.; Ariga, K.; Nakahara, H.; Fukuda, K. *J. Chem. Soc., Chem. Commun.* **1986**, 1069.

(3) (a) Kajiyama, T.; Kumano, A.; Takayanagi, M.; Okahata, Y.; Kunitake, T. *Chem. Lett.* **1979**, 645. (b) Kumano, A.; Kajiyama, T.; Takayanagi, M.; Kunitake, T.; Okahata, Y. *Ber. Bunsen-Ges. Phys. Chem.* **1984**, *88*, 1216.

(4) (a) Sada, E.; Katoh, S.; Teranishi, M. *Biotechnol. Bioeng.* **1983**, *25*, 317. (b) Sada, E.; Katoh, S.; Teranishi, S.; Takeda, Y. *AIChE J.* **1985**, *31*, 311.

(5) Araki, K.; Konno, R.; Seno, M. *J. Membr. Sci.* **1984**, *17*, 89.

(6) Vanderveen, R. J.; Barnes, G. T. *Thin Solid Films* **1985**, *134*, 227.

(7) (a) Kunitake, T.; Higashi, N.; Kajiyama, T. *Chem. Lett.* **1984**, 717. (b) Higashi, N.; Kunitake, T.; Kajiyama, T. *Macromolecules* **1986**, *19*, 1362.

(8) (a) For a review, see: Okahata, Y. *Acc. Chem. Res.* **1986**, *19*, 57. (b) Okahata, Y.; Ariga, K.; Seki, T. *J. Am. Chem. Soc.* **1988**, *110*, 2495.

(9) Okahata, Y.; Taguchi, K.; Seki, T. *J. Chem. Soc., Chem. Commun.* **1985**, 1122. Okahata, Y.; Fujita, S.; Iizuka, N. *Angew. Chem., Int. Ed. Engl.* **1986**, *25*, 751. Okahata, Y.; En-na, G. *J. Phys. Chem.* **1988**, *92*, 4546. Okahata, Y.; Takenouchi, K. *Macromolecules* **1988**, *22*, 308.

(10) Blodgett, K. B. *J. Am. Chem. Soc.* **1935**, *57*, 1007.

(11) Blodgett, K. B.; Langmuir, I. *Phys. Rev.* **1937**, *51*, 964.

(12) Albrecht, O.; Laschewsky, A.; Ringsdorf, H. *Macromolecules* **1984**, *17*, 937. Albrecht, O.; Laschewsky, A.; Ringsdorf, H. *J. Membr. Sci.* **1985**, 22, 187.

(13) Rose, G. D.; Quinn, J. A. *J. Colloid Interface Sci.* **1968**, *27*, 193.

(14) Gaines, G. L.; Ward, W. J. *J. Colloid Interface Sci.* **1977**, 60, 210.

(15) Higashi, N.; Kunitake, T.; Kajiyama, T. *Polym. J.* **1987**, *19*, 289.

(16) Higashi, N.; Kunitake, T.; Kajiyama, T. *Kobunshi Ronbunshu (Tokyo)* **1986**, *43*, 761.

(17) Kajiyama, T.; Kumano, A.; Takayanagi, M.; Kunitake, T. *Chem. Lett.* **1984**, 915.

(18) Heckmann, K.; Strobl, CH.; Bauer, S. *Thin Solid Films* **1983**, *99*, 265.

(19) Cackovic, H.; Schwengers, H.-P.; Springer, J.; Laschewsky, A.; Ringsdorf, H. *J. Membr. Sci.* **1986**, *26*, 63.

0002-7863/89/1511-5618$01.50/0